

3D HD AND MHD ADAPTIVE MESH REFINEMENT SIMULATIONS OF THE GLOBAL AND LOCAL ISM

Miguel A. de Avillez¹ and Dieter Breitschwerdt²

¹*Department of Mathematics, University of Évora, R. Romão Ramalho 59, 7000 Evora, Portugal, Email: mavillez@galaxy.lca.uevora.pt*

²*Institut für Astronomie, Universität Wien, Türkenschanzstr. 17, A-1180 Wien, Austria, Email: breitschwerdt@astro.univie.ac.at*

Abstract We have performed high resolution 3D simulations with adaptive mesh refinement, following the ISM evolution in a star forming galaxy both on small (<1 pc) and large (>10 kpc) scales, enabling us to track structures in cooling shock compressed regions as well as the entire Galactic fountain flow. It is shown in an MHD run that the latter one is not inhibited by a large scale disk parallel magnetic field. The fountain plays a vital rôle in limiting the volume filling factor of the hot gas. Contrary to classical models most of the gas between 100K and 8000 K is found to be thermally unstable. On scales of superbubbles we find that the internal temperature structure is rather inhomogeneous for an old object like our Local Bubble, leading to low OVI column densities, consistent with observations.

Keywords: Hydrodynamics and Magnetohydrodynamics, ISM: kinematics and dynamics, ISM: structure, Local Bubble, OVI column densities

1. Introduction

In their seminal paper of a three-phase model regulated by supernova explosions in an inhomogeneous medium, [21] predicted a volume filling factor of the hot intercloud medium (HIM) of $f_{v,hot} \simeq 0.7 - 0.8$. However, observations point to a value of ~ 0.5 (e.g., [13]) or even lower when external galaxies are taken into account (e.g., [10]). A way out has been suggested by [22] by the so-called chimney model, in which hot gas can escape into the halo through tunnels excavated by clustered supernova (SN) explosions. Indeed X-ray observations of several nearby edge-on galaxies have revealed extended, galaxy-sized halos (e.g., [27]). The transport of gas into the halo is, however, still controversial, since break-out may be inhibited by a large-scale disk parallel magnetic field (see e.g., [23]). However, [26] has performed 3D MHD simulations of expanding superbubbles, including radiative cooling, and finds

that bubble confinement only occurs when the energy injection rate is below a critical value of $\sim 10^{37}$ erg s $^{-1}$ (see also [20]) and/or the field scale height is infinite, which is unrealistic.

Attempts to determine the occupation fraction of the different phases, and in particular of the hot gas, by means of modelling the effects of SNe and SBs in the ISM, have been carried out by several authors (e.g., [14, 15, 19]). However, these models do not include the circulation of gas between the disk and the *full* halo, thus being unable to resolve the high- z region; neither do they take into account the mixing between the different phases. Therefore, an estimate of the volume filling factors may be misleading. Using the 3D supernova-driven ISM model of [2] incorporating magnetic fields and the adaptive mesh refinement technique in HD [1] and MHD (using a modified version of [8]) algorithms coupled to a 3D parallel (multi-block structured) scheme, we explored the effects of the establishment of the disk-halo-disk circulation and its importance for the evolution of the ISM in disk galaxies both with and without magnetic fields. In this paper we review some of the results from these simulations (§3), and compare in the case of the Local Bubble derived OVI column densities with observations (§4), followed by a discussion of the dynamical picture that emerges from these simulations. Other important issues like the volume filling factors of the ISM "phases", the dynamics of the galactic fountain, the conditions for dynamical equilibrium and the importance of convergence of these results with increasing grid resolution, the variability of the magnetic field with density, the importance of ram pressure in the ISM, and the amount of gas in the unstable regimes have been treated elsewhere [2–6].

2. Model and Simulations

We ran HD and MHD simulations of the ISM on scales of kpc, driven by SNe at the Galactic rate, on a Cartesian grid of $0 \leq (x, y) \leq 1$ kpc size in the Galactic plane and $-10 \leq z \leq 10$ kpc in the halo with a finest adaptive mesh refinement resolution of 0.625 pc (for the HD run) and 1.25 pc (for the MHD run) starting from a resolution of 10 pc, using a modified version of the 3D model of [2], fully tracking the time-dependent evolution of the large scale Galactic fountain for a time sufficiently long so that the memory of the initial conditions is completely lost, and a global dynamical equilibrium is established.

The model includes the gravitational field provided by the stellar disk, radiative cooling (assuming an optically thin gas in collisional ionization equilibrium) with a temperature cut off at 10 K, and uniform heating due to starlight varying with z . In the Galactic plane background heating is chosen to initially balance radiative cooling at 9000 K. With the inclusion of background heating the gas at $T < 10^4$ K becomes thermally bistable. The prime sources of mass, momentum and energy are supernovae types Ia, Ib+c and II with scale heights,

distribution and rates taken from the literature. OB associations form in regions with density $n \geq 10 \text{ cm}^{-3}$ and temperature $T \leq 100 \text{ K}$. The number, masses and main sequence life times (τ_{MS}) of the stars in the association are determined from the initial mass function (IMF). At the end of τ_{MS} the stars explode. The stars from the OB association that turn into supernovae in the field have their locations determined kinematically by attributing to each star a random direction and a velocity at the time of their formation. The canonical explosion energy is 10^{51} erg for all types of SNe. The interstellar gas initially has a density stratification distribution that includes the cold, cool, warm, ionized and hot “phases” in the Galaxy as described in, e.g., [15]. The magnetic field has uniform and random components, initially given by $B_u = (B_{u,0}(n(z)/n_0)^{1/2}, 0, 0)$ and $B_r = 0$, respectively, where $B_{u,0} = 3 \mu\text{G}$ is the field strength, $n(z)$ is the number density of the gas as a function of distance from the Galactic midplane, and $n_0 = 1 \text{ cm}^{-3}$ is the average midplane density. This random component of the field is built up during the first millions of years of evolution as a result of turbulent motions, mainly induced by SN explosions. The total magnetic field strength at any time $t > 0$ is given by $\sqrt{B_u^2 + B_r^2} > 3 \mu\text{G}$.

3. Results

Global Evolution. The initial evolution of the magnetized disk is similar to that seen in the HD run, that is, the initially stratified distribution does not hold for long as a result of the lack of equilibrium between gravity and (thermal, kinetic and turbulent) pressure during the “switch-on phase” of SN activity. As a consequence the gas in the upper and lower parts of the grid collapses onto the midplane, leaving low density material in its place. However, in the MHD run the collapse takes longer due to the opposing magnetic pressure and tension forces. As soon as enough supernovae have gone off in the disk building up the required pressure support, transport into the halo is not prevented, although the escape of the gas takes a few tens of Myr to occur. The crucial point is that a huge thermal overpressure due to combined SN explosions can sweep the magnetic field into dense filaments and punch holes into the extended warm and ionized HI layers. Once such pressure release valves have been set up, there is no way from keeping the hot over-pressured plasma to follow the density gradient into the halo. As a consequence the disk-halo-disk duty cycle of the hot gas is fully established, in which the competition of energy input and losses into the ISM by SNe, diffuse heating and radiative cooling leads the system to evolve into a dynamical equilibrium state within a few hundred Myr. This time scale is considerably longer than that quoted in other papers (e.g., [19], [18]), because in these the galactic fountain has not been taken into account.

Summary of Main Results. The simulations show that:

(i) the highest density gas tends to be confined to shocked compressed layers that form in regions where several large scale streams of convergent flow (driven by SNe) occur. The compressed regions, which have on average lifetimes of 10-15 Myr, are filamentary in structure, tend to be aligned with the local field and are associated with the highest field strengths (in the MHD run), while in the HD runs there is no preferable orientation of the filaments. The formation time of these high density structures depends on how much mass is carried by the convergent flows, how strong the compression and what the rate of cooling of the regions under pressure are;

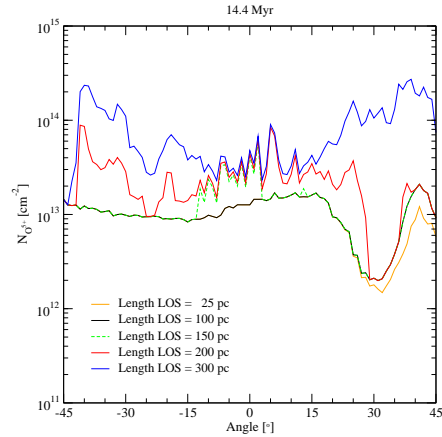
(ii) the volume filling factors of the different ISM phases depend sensitively on the existence of a duty cycle between the disk and halo working as a pressure release valve for the hot ($T > 10^{5.5}$ K) phase in the disk. The mean occupation fraction of the hot phase varies from about 15% for the Galactic SN rate to $\sim 30\%$, for $\sigma/\sigma_{Gal} = 4$, and to 52% for $\sigma/\sigma_{Gal} = 16$ (corresponding to a starburst). Overall the filling factor of the hot gas does not increase with SN rate as much as may be expected, since due to the evacuation of the hot phase into the halo through the duty cycle it never exceeds much more than about half of the disk volume (see also [3]);

(iii) with the magnetic field present and initially orientated parallel to the disk varying as $\rho^{1/2}$, transport into the halo is inhibited but not prevented. As a consequence the hot gas in the disk has a volume filling factor similar to that in the corresponding HD simulation (i.e., $\leq 20\%$);

(iv) the magnetic field has a high variability and it is *largely uncorrelated with the density* suggesting that it is driven by inertial motions (which is consistent with the dominance of the ram pressure - see below), rather than it being the agent determining the motions. In the latter case the field would not be strongly distorted, and it would direct the motions predominantly along the field lines. Therefore the classical scaling law $B \sim \rho^{1/2}$ according to the Chandrasekhar-Fermi (CF) model (1953, [11]) does not hold contrary to what has been claimed by [18]. We suspect that this discrepancy can be explained by the $(200 \text{ pc})^3$ box that these authors have used, centered in the Galactic midplane with periodic boundary conditions in all the box faces; thus they have missed completely the disk-halo disk circulation and did not allow for a global dynamical equilibrium to be established (see [6] for a detailed discussion).

(v) Ram pressure controls the flow for $10^2 < T \leq 10^6$ K. For $T > 10^6$ K thermal pressure dominates, while for $T \leq 10^2$ K (thermally stable branch) magnetic pressure takes over. Near supernovae thermal and ram pressures determine the dynamics of the flow. The hot gas in contrast is controlled by the thermal pressure, since magnetic field lines are swept towards the dense compressed walls. Up to 80% of the mass in the disk is concentrated in the classical thermally *unstable* regime $10^2 < T \leq 10^{3.9}$ K with $\sim 60\%$ of the warm neutral medium (WNM) mass enclosed in the $500 \leq T \leq 5000$ K gas. This result

is in contradiction with the standard ISM theory [21], but strongly supported by recent 21cm line observations of the warm neutral medium [16], who find a fraction $\geq 48\%$ in this unstable temperature range. We conclude that SN driven shocks and ensuing turbulence are capable of replenishing gas in the thermally unstable branches by constantly stirring up the ISM.



Left: mavillez_.fig1a.jpeg

Figure 1. *Left:* Temperature map (cut through Galactic plane) of a 3D Local Bubble simulation at 14.4 Myr after the first explosion showing the LB centered at (175, 400) pc and Loop I centered at 200 pc to the right along the straight line. *Right:* OVI column density varying over the angles $\pm 45^\circ$ for different LOS path lengths.

4. Does the SN Driven ISM Model hold on smaller scales?

In the previous sections we have demonstrated how the interstellar matter cycle works on global scales. How about smaller ones? Let us look for the remainder of this paper at local superbubbles, i.e. the Local and Loop I bubbles, and, more specifically, at the OVI column density in absorption, which is a crucial test for modelling (cf. [12]). We therefore carried out a run for the Local Bubble and Loop I following the work by [7], who suggested that the LB was created by successive explosions of stars from the moving subgroup B1 of the Pleiades in the last 15 Myrs. We used data cubes of previous runs with a finest AMR resolution of 1.25 pc taken after the global dynamical equilibrium has been established and followed the trajectory of the moving group having 20 stars with masses between 11 and 20 M_\odot as predicted by the IMF derived in [7]. This run over 20 Myrs with boundary conditions discussed in §2, followed the effects of the 20 and 39 SN explosions, respectively, in the LB and Loop I bubbles. The SNe in the LB went off along a path crossing the arbitrarily chosen location at (175, 400) pc, whereas Loop I is powered by explosions in the Sco

Cen Association, located here at (375, 400) pc (left panel of Fig. 1). These SNe generated the cavities in which the LB and Loop I expand. The Galactic supernova rate has been used for the setup of *other SNe* in the remaining disk as a realistic background medium, in to which the bubbles expand.

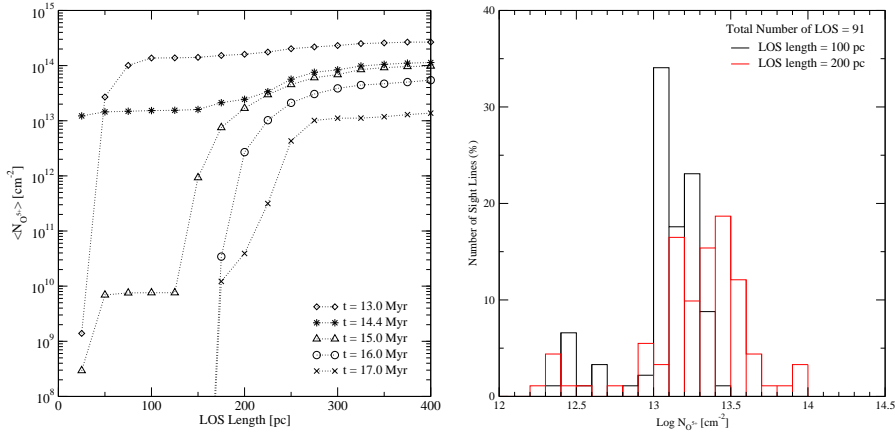


Figure 2. *Left:* OVI column density averaged over angles indicated in Fig. 1 as a function of LOS path length at 13, 14.4, 15, 16 and 17 Myr of Local and Loop I bubbles evolution. *Right:* Histogram showing the percentage of LOS within various ranges of observed column density for different LOS path lengths at 14.4 Myr.

The locally enhanced SN rate produces a coherent LB structure within a highly disturbed background medium (due to ongoing star formation). Successive explosions heat and pressurize the LB, which at first looks smooth, but develops internal structure at $t > 8$ Myr. After 14 Myr the 20 SNe that occurred inside the LB fill a volume roughly corresponding to the present day LB (Fig. 1). The LB is still bounded by a shell, which will start to fragment due to Rayleigh-Taylor instabilities in ~ 3 Myr from now. This will lead to mass transfer of hot gas from Loop I to the Local Bubble, and in ~ 10 Myr the bubbles will merge. Clouds and cloudlets of various sizes are formed when the dense shells of the bubbles collide, as has been predicted by [9]. The volume filling factor of the hot ambient gas in this run is still moderately low ($\sim 18\%$).

The right panel of Fig. 1 shows the OVI column density measured through lines of sight (LOS) with different lengths that run from 0° (along x -axis) to $\pm 45^\circ$ (pos. angles counterclockwise) as shown in the left panel of the same figure. These LOS all cross or point towards Loop I (the hot pressured region located to the right of the LB). The column density within the LB varies between 10^{12} and $2.1 \times 10^{13} \text{ cm}^{-2}$, while for LOS sampling gas from outside the LB (i.e., ahead 100 pc) the column density is in the range 10^{13} cm^{-2} and $3 \times 10^{14} \text{ cm}^{-2}$. The average column density of OVI ($\langle N_{O^{5+}} \rangle$) for 14.4 Myr varies between

$1.5 \times 10^{13} \text{ cm}^{-2}$ and $1.4 \times 10^{14} \text{ cm}^{-2}$ for a LOS length l_{LOS} of 100 and 400 pc, respectively (left panel of Fig. 2). Within the LB $\langle N_{O^{5+}} \rangle$ decreases steeply with time for $t > 14.4 \text{ Myr}$, because no further SN explosions occur. The right panel of Fig. 2 shows the histogram of the percentage of lines of sight within various ranges of observed column density for different l_{LOS} . For $l_{LOS} = 100 \text{ pc}$ there are two strong peaks: one at $1.3 \times 10^{13} \text{ cm}^{-2}$ and another at $1.6 \times 10^{13} \text{ cm}^{-2}$ from absorbing gas inside the LB. This second peak is consistent with the fact that the main contribution for the OVI column density comes from the LB as discussed by [25], who inferred an average value of $1.6 \times 10^{13} \text{ cm}^{-2}$ from analysis of COPERNICUS absorption line data.

5. Conclusions

The dynamical picture that emerges from these simulations is that the evolution of the ISM in disk galaxies is intimately related to the vertical structure of the thick gas disk and to the energy input per unit area by supernovae. The system evolves towards a dynamical equilibrium state on the global scale if the boundary conditions vary only in a secular fashion. Such an equilibrium is determined by the input of energy into the ISM by SNe, diffuse heating, the energy lost by radiative and adiabatic cooling and magnetic compression, and is only possible *after* the full establishment of the Galactic fountain, which for the Milky Way takes about 300 Myr ([3], see also [17]). It should be emphasized, since disk and halo are dynamically coupled not only by the escape of hot gas, but also by the fountain *return* flow striking the disk, that the disk equilibrium will also suffer secular variations (see also [24]).

Furthermore, the ISM in the disk is dominated by thermal pressure gradients mostly in the neighborhood of SNe, which drive motions whose ram pressures are dominant over the mean thermal pressure (away from the energy sources) and the magnetic pressure. The magnetic field is only dynamically important at low temperatures, but can also weaken gas compression in MHD shocks and hence lower the energy dissipation rate. The thermal pressure of the freshly shock heated gas exceeds the magnetic pressure by usually more than an order of magnitude and the B-field can therefore not prevent the flow from rising perpendicular to the galactic plane. Thus, the hot gas is fed into the galactic fountain at almost a similar rate than without field.

On the scales of superbubbles, it is found that their expansion into a highly turbulent and inhomogeneous medium leads to considerable deviations from the classical model by developing internal temperature and density structure for older bubbles. Thus the OVI column densities we find there are fairly low – and in agreement with observations – while to our knowledge other Local Bubble models so far have failed this test.

Acknowledgments

MAdeA is partly supported by the Portuguese Science Foundation (FCT) through the FAAC fund. This work has been partially funded by FCT under the project PESO/P/PRO/40149/2000 to MAdeA and DB.

References

- [1] Avillez, M. A.: 1998, Ph.D. Thesis, University of Évora, Portugal.
- [2] Avillez, M. A.: 2000, *MNRAS*, 315, 479.
- [3] Avillez, M. A. and Breitschwerdt, D.: 2004, *A&A*, in press.
- [4] Avillez, M. A. and Breitschwerdt, D.: 2004, *Ap&SS*, in press (Astro-ph/0310633).
- [5] Avillez, M. A. and Breitschwerdt, D.: 2004, *Ap&SS*, in press (Astro-ph/0310634).
- [6] Avillez, M. A. and Breitschwerdt, D.: 2004, *Baltic Astronomy*, in press (Astro-ph/0311394).
- [7] Berghöfer, T. and Breitschwerdt, D.: 2002, *A&A* **390**, 299.
- [8] Balsara, D. S.: 2001, *JCP* **174**, 614.
- [9] Breitschwerdt D., Freyberg, M.J., Egger R.: 2000, *A&A* **361**, 301.
- [10] Brinks, E. and Bajaja, E.: 1986, *A&A* **169**, 14.
- [11] Chandrasekhar, S. and Fermi, E.: 1953, *ApJ* **118**, 113.
- [12] Cox, D.P.: 2004, *ApSS*, in press (Astro-ph/0302470).
- [13] Dettmar, R.-J.: 1992, *Fund. of Cosm. Phys.*, 15, 143.
- [14] Ferrière, K.M.: 1995, *ApJ* **441**, 281.
- [15] Ferrière, K.M.: 1998, *ApJ* **503**, 700.
- [16] Heiles, C. and Troland, T.H.: 2003, *ApJ* **586**, 1067.
- [17] Kahn F.D.: 1981, in: F.D. Kahn (ed.), *Investigating the Universe*, Reidel, Dordrecht, p. 1.
- [18] Kim, J., Balsara, D. and Mac Low M.-M.: 2001, *JKAS* **34**, S333.
- [19] Korpi, M.J., Brandenburg, A., Shukurov, A., Tuominen, I. and Nordlund, A.: 1999, *ApJ* **514**, L99.
- [20] MacLow, M.-M. and McCray, R.: 1988, *ApJ* **324**, 776.
- [21] McKee, C.F. and Ostriker, J.P.: 1977, *ApJ* **218**, 148.
- [22] Norman, C.A. and Ikeuchi, S.: 1989, *ApJ* **345**, 372.
- [23] Mineshige, S., Shibata, K. and Shapiro, P.R.: 1993, *ApJ* **409**, 663.
- [24] Rosen, A. and Bregman, J.N.: 1995, *ApJ* **440**, 634.
- [25] Shelton, R. and Cox, D.P.: 1994, *ApJ*, **434**, 599.
- [26] Tomisaka, K.: 1998, *MNRAS* **298**, 797.
- [27] Wang, Q.D., Immler, S., Walterbos, R., Lauroesch, J.T. and Breitschwerdt, D.: 2001, *ApJ* **555**, L99.

This figure "mavillez_fig1a.jpeg" is available in "jpeg" format from:

<http://arxiv.org/ps/astro-ph/0402448v1>